Ab Initio Reaction Path Analysis of Benzene Hydrogenation to Cyclohexane on Pt(111)†

Mark Saeys,‡,|| M.-F. Reyniers,‡ M. Neurock,§ and G. B. Marin*,‡

Laboratorium voor Petrochemische Techniek, Ghent University, Krijgslaan 281(S5), B-9000 Gent, Belgium, and Department of Chemical Engineering, University of Virginia, 102 Engineers' Way, Charlottesville, Virginia 22904-4741

Received: February 9, 2004; In Final Form: April 19, 2004

First-principles density functional theory calculations were performed to obtain detailed insight into the mechanism of benzene hydrogenation over Pt(111). The results indicate that benzene hydrogenation follows a Horiuti-Polanyi scheme which involves the consecutive addition of hydrogen adatoms. A first-principles-based reaction path analysis indicates the presence of a dominant reaction path. Hydrogenation occurs preferentially in the meta position of a methylene group. Cyclohexadiene and cyclohexene are expected to be at best minor products, since they are not formed along the dominant reaction path. The only product that can desorb is cyclohexane. Along the dominant reaction path, two categories of activation energies are found: lower barriers at ∼75 kJ/mol for the first three hydrogenation steps, and higher barriers of ∼88 kJ/mol for steps four and six, where hydrogen can only add in the ortho position of two methylene groups. The highest barrier at 104 kJ/mol is calculated for the fifth hydrogenation step, which may potentially be the rate-determining step. The high barrier for this step is likely the result of a rather strong C−H···Pt interaction in the adsorbed reactant state (1,2,3,5-tetrahydrobenzene*) which increases the barrier by ∼15 kJ/mol. Benzene and hydrogen are thought to be the most-abundant reaction intermediates.

1. Introduction

The hydrogenation of benzene over transition metal catalysts is the archetypical model probe reaction that is used to test the aromatic hydrogenation functionality of the catalyst. In addition, the hydrogenation of benzene as well as other aromatics is industrially relevant for a number of critical steps in petroleum refining and downstream chemical processing. Fuel quality as well as environmental concerns continue to impose stricter limits on the aromatic content of fuels.[1] Also for the production of cyclohexane, a base chemical for nylon 6,6, benzene hydrogenation is the major process. Moreover, hydrogenation reactions have been found to be structure-insensitive;[2] therefore studies on model surfaces can provide valuable information, applicable to real industrial catalysts. For these reasons, many kinetic and surface science studies have addressed the hydrogenation of benzene, as well as the adsorption and dehydrogenation of the possible reaction intermediates, cyclohexadiene, cyclohexene and cyclohexane.[5−34]

Despite this large database of experimental studies, a detailed picture of the mechanism of benzene hydrogenation is still lacking. The rather large number of hydrogenation steps results in a large number of possible reaction paths. This complexity is illustrated in Figure 1. Earlier studies indicate that benzene hydrogenation follows a Horiuti-Polanyi mechanism,[35] i.e., hydrogenation occurs sequentially. Various kinetic models have been proposed to capture the kinetics for the hydrogenation of aromatics. Most kinetic models assume a sequence of hydrogen addition steps, from benzene to cyclohexadiene to cyclohexene and to cyclohexane, though from Figure 1 it is clear that alternative pathways are also possible. On the basis of radiotracer studies, Paal and Tetenyi suggest that hydrogenation proceeds in a random fashion[4] or via a reaction path that does not pass via cyclohexene.[3] Experimentally, little cyclohexene formation is observed during benzene hydrogenation over transition metal catalysts, except for Ru-based processes,[36] consistent with the reaction path proposed by Tetenyi and Paal.[3] Actually, for the six sequential hydrogenation steps in benzene hydrogenation, 14 possible reaction paths can be proposed (Figure 1). The actual number of possible reaction paths is even higher (about 180), since the symmetry of the adsorbed species is lower than the symmetry of the gas-phase molecules.

In addition to the complexity of the reaction network, there is no concensus on the nature of the rate-determining step for this process. Some researchers propose that the addition of the first hydrogen is the rate-determining step, since it "breaks the aromaticity" (e.g., ref 5), while others suggest that the fourth step may be rate-determining.[6] Other studies have proposed a kinetic model without invoking a rate-determining step[6−8] or allowed for a linear distribution of activation energies between the first and the sixth hydrogenation step.[9]

The large number of possible reaction paths makes it difficult to put forward a most likely reaction path and establish the presence and location of a rate-determining step based on chemical intuition alone. Hence, a substantial number of possible rate equations can be postulated. This makes model discrimination based on experimental data very difficult. Over the past decade, surface science studies on ideal (111) surfaces and more realistic model catalysts, in combination with theoretical results based on density functional theory, have provided detailed insight into the mechanism of ethene hydrogenation.[2,37−39] The

† Part of the special issue "Michel Boudart Festschrift".

* Corresponding author. Tel: ++32 9 2644516. Fax: ++32 9 2644999. E-mail: Guy.Marin@UGent.be.

‡ Ghent University.

§ University of Virginia.

|| Present address: Department of Chemical and Biomolecular Engineering, National University of Singapore, 4 Engineering Drive 4, Singapore 117576

10.1021/jp049421j CCC: $30.25
Published on Web 05/29/2004

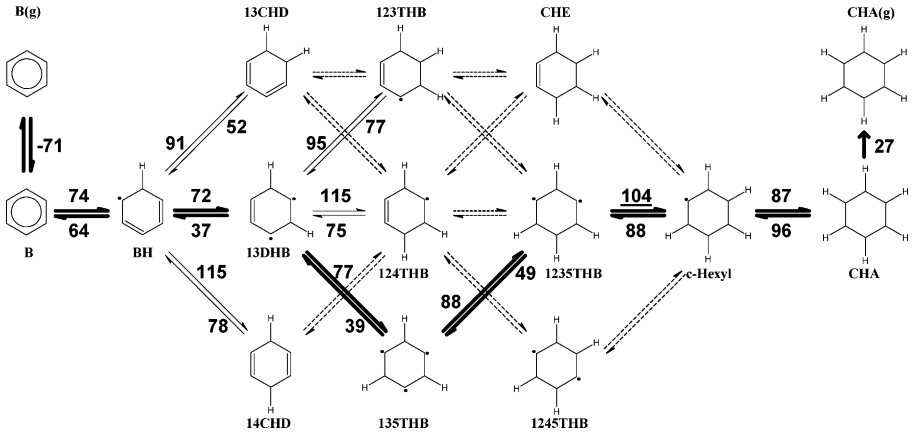

Figure 1. Possible reaction paths for the hydrogenation of benzene to cyclohexane. Possible reactive intermediates are indicated with the acronyms that are used in this text. The dominant reaction path is indicated in boldface. The calculated hydrogenation and dehydrogenation activation energies are indicated. The energy values are given in kJ/mol.

success of this approach has motivated us to try to elucidate the complex mechanism of benzene hydrogenation using a reaction path analysis based on DFT calculations.

Previously, we have studied the adsorption of benzene[10] and 1,4-cyclohexadiene[11] on Pt(111), as well as the first two hydrogenation steps of benzene to cyclohexadiene and the dehydrogenation of benzene[12] in detail using cluster DFT calculations. The results of these first principles studies were compared directly and indirectly to surface science data, showing qualitative as well as quantitative agreement. These theoretical benchmark studies indicate that the selected theoretical procedure can be used with some confidence to study the full reaction path from benzene to cyclohexane.

A number of fundamental concepts for the analysis of catalytic reaction mechanisms were introduced and reviewed recently by Boudart.[43] These concepts are the following: the catalytic cycle; the rate-determining step (RDS) for a reaction which is "far from equilibrium" in the catalytic cycle as compared to the other steps in the mechanism; and the most-abundant reaction intermediate (MARI) which allows a simplification of the site balance. Here, we will use ab initio density functional theory to assess these concepts for the construction of a fundamental kinetic model for the hydrogenation of monoaromatic molecules. In particular, the following questions will be addressed:

- From the many possible reaction paths, is there a dominant path along which activation energies are lower than along any other or does hydrogen addition occur in a random fashion?
- Along the dominant reaction path, can a RDS be located?
- From an analysis of the enthalpy profile along the dominant reaction path, is there a reaction intermediate significantly more stable, so that it can be considered the MARI?

2. Computational Methodology

The selection of an adequate quantum chemical method for modeling adsorption and reaction on the catalyst surface is not an easy task and is limited by the accuracy that one can gain in a higher level theoretical treatment at the expense of the loss of description of the catalytic surface. An optimal ab initio approach to the study of the hydrogenation of benzene was found to be relativistic density functional theory (DFT) with the Becke Perdew (BP86) functional[44] which enables us to examine Pt clusters large enough to contain the adsorption site as well as the local coordination about the active site. Scalar relativistic effects were included through the zero-order regular approximation (ZORA) Hamiltonian.[45] Basis sets were of double-ζ quality and constructed from Slater type orbitals (STO). The innermost atomic shells were kept frozen and replaced by a fully relativistic core density. The Pt(111) catalyst was modeled by a two-layered Pt_{22} cluster with 14 atoms in the top layer. The Pt−Pt distance was constrained at the bulk value of 277 pm.[46] Adsorption and reaction were studied on the central atoms of the top layer of this cluster. All these calculations were carried out using the Amsterdam density functional (ADF2000) computational program.[45] In previous publications we have demonstrated that this approach yields reasonably accurate values for benzene,[10] cyclohexadiene,[11,13] and cyclohexene[13] adsorption enthalpies, as well as for cyclohexadiene dehydrogenation activation energies,[12] both in comparison with fully periodic slab calculations or with experimental data. The accuracy of DFT for the prediction of adsorption energies and activation energies is often stated to be within 10−20 kJ/mol of reported experimental values, though relative values are often found to be more accurate.[2]

Transition state structures were located in four steps. First, a series of calculations is performed to map out a portion of the potential energy surface. This is done by examining a series of structures along the linear transient between the reactant and product states. The reaction path involves the breaking of Pt−C and Pt−H bonds and the formation of a C−H bond. A series of states that lie at ∼10 pm increments along the linear path between the reactant and product state was chosen as starting structures to examine the potential energy surface. The C−H distance is constrained at each of these steps, while all other internal coordinates are optimized. This leads to a first-order approximation of the transition state geometry. The resulting geometry is then used as input to a more rigorous eigenmode following search strategy to isolate a true transition state. At this point, it is checked that the Hessian has one and only one negative eigenvalue. To verify the transition state that was located indeed corresponds to the desired reaction, the path from the transition state to the products and to the reactants was traced, using the intrinsic reaction coordinate method. To gain computational efficiency, up to this point all the calculations were performed on smaller constrained model clusters. The resulting transition state geometry is then used as an initial guess in an eigenmode following transition state optimization on the large Pt_{22} model cluster. The approximate Hessian of the resulting transition state is verified to have one and only one negative eigenvalue.

Accurate reference gas-phase enthalpies of formation for the reaction intermediates were calculated using the atom additivity

TABLE 1: Gas-Phase Enthalpy of Formation and Adsorption Energies for Different Possible Reaction Intermediates (kJ/mol)

molecule[a]	BP86[b]	CBS-QB3*	expt[50]	calculated adsorption energy
B	83	82	**82.9** ± 0.5	−102 (bridge)
				−71 (hollow)
H_2	0		0.0	−94 (top)
				−85 (hollow)
H	231		218	−265 (top)
				−261 (hollow)
BH	187	204		−229
13CHD	79	**110**	104.6 ± 0.7	−155 (bridge, 1,2-π−3,4-di-σ)
				−147 (hollow)
				−75 (bridge, 2,3-π−1,4-di-σ)
14CHD	84	**111**	100.4 ± 3.1; 109	−146 (bridge)
				−142 (hollow)
				−88 (bridge, di-π)
13DHB	285	325		−370
123THB	76	128		−203
124THB	143	194		−254
135THB	411	472		−526
CHE	−64	−3	**−4.3** ± 1.0	−81 (boat di-σ)
1235HB	204	271		−333
1245HB	201	275		−298
c-hexyl	−7	74		−167
CHA	−214	−124	**−123.1** ± 0.8	−27 (hollow)

[a] The acronyms refer to Figure 1. [b] ΔH_f were calculated from the standard reaction enthalpy of $B + {}^{x}/_{2}H_2 \rightarrow BH_x$, using the experimental ΔH_f values of gas-phase benzene and hydrogen.

corrected CBS-QB3 method.[47,48] These calculations were performed with the Gaussian98 quantum chemistry program.[49]

3. Results and Discussion

This section has been split into two parts. In the first part, the adsorption enthalpies of the different possible reaction intermediates and the resulting reaction enthalpy diagram are discussed. The adsorption enthalpies are compared with available experimental values. Analysis of the enthalpy diagram may provide some information about possible rate-determining steps and most-abundant reaction intermediates (MARI). In the second part, we present ab initio activation energies to further discriminate between the possible reaction paths and assess potential rate-determining steps.

3.1. Enthalpy Diagram. Most theoretical studies of catalytic reactions use DFT *energies* to map the *enthalpy* diagram of the reaction. For reactions such as benzene hydrogenation which consist of a significant number of consecutive elementary steps, the neglect of zero-point energies and to some extent of thermal corrections may lead to an important accumulation of errors in the calculation of the reaction enthalpies. The accuracy of the enthalpy diagram can be substantially improved by using accurate gas-phase enthalpies of formation for the reaction intermediates as reference points. For some of the reaction intermediates in Figure 1, accurate experimental enthalpies of formation are available. However, for many of the radical species, experimental data are lacking. For these species, accurate enthalpies of formation can be calculated using the atom additivity corrected CBS-QB3 method, CBS-QB3*.[47,48] Previously, it was demonstrated that the CBS-QB3* method succeeds in predicting standard enthalpies of formation of hydrocarbons with a mean absolute deviation (MAD) of 2.5 kJ/mol.[47] Table 1 lists the standard gas-phase enthalpies of formation for the reaction intermediates. The abbreviations used in Table 1 correspond to the definitions given in Figure 1. To illustrate the potential deviations that can result when using DFT *energies* to map the *enthalpy* diagram, the BP86 values are also given. Deviations up to 90 kJ/mol (cyclohexane) can be found. For benzene (B), cyclohexadiene (13CHD and 14CHD), cyclohexene (CHE), and cyclohexane (CHA), both CBS-QB3* and experimental values are listed. For B, CHE and CHA, the CBS-QB3* values are in good agreement with the experimental data. For these molecules we prefer to use the experimental values, since the reported experimental uncertainty is better than the MAD of the CBS-QB3* method. For 14CHD, two inconsistent experimental values were found.[50] The higher value is in good agreement with the ab initio value, but the lower value deviates significantly. We therefore prefer using the CBS-QB3* enthalpy of formation for 14CHD. Also for 13CHD, we prefer to use the CBS-QB3* values, to be consistent with the nearly thermoneutral cyclohexadiene isomerization enthalpy.[50] For the radical intermediates no experimental enthalpies of formation were found in the NIST Chemistry WebBook.[50]

Next, adsorption energies will be reported for the possible reaction intermediates. In combination with the accurate standard gas-phase enthalpies of formation of Table 1, a reaction enthalpy diagram can be constructed using eq 1

$$\Delta H_r(\text{surface}) = \Delta H_r(\text{gas phase}) - E_{ads}(\text{react,DFT}) + E_{ads}(\text{prod,DFT}) \quad (1)$$

where ΔH_r(surface) is the surface reaction enthalpy, ΔH_r(gas phase) is the experimental or CBS-QB3* ab initio gas-phase reaction enthalpy and E_{ads}(X,DFT) is the DFT ab initio adsorption *energy* for X.

The adsorption of cyclic C_6 molecules has been the subject of a number of surface science and DFT studies.[10−34] In particular, the adsorption of stable molecules—hydrogen, benzene, CHD, CHE, and CHA—has received considerable attention. In the following discussion we will mainly focus on these species. For most of the molecules, different adsorption modes have been found both experimentally and theoretically. Ab initio calculations can help to elucidate the sometimes complicated adsorption behavior. The experimental data also allow a validation of the selected theoretical approach. However, since the focus of this paper is the reaction path analysis, we will only review the major conclusions of the adsorption studies and discuss the resulting enthalpy diagram in more detail. A more in-depth discussion of the adsorption process can be found elsewhere.[10,11,13]

Benzene adsorption is the first step of the hydrogenation reaction path and was studied extensively.[10] Benzene was found to adsorb at two sites on the Pt(111) surface: at the bridge(0) and the hollow(30) site with adsorption energies of −102 and −71 kJ/mol, respectively. Temperature-programmed desorption studies have also reported two adsorption modes with adsorption energies around −120 and −85 kJ/mol.[14] Recently, Morin et al.[16] studied benzene adsorption on Pt(111) using periodic DFT calculations on a large six-layered slab model. Their best adsorption energies of, respectively, −100 and −73 kJ/mol for the bridge and the hollow site are in excellent agreement with our findings. Thermodynamic considerations and comparison of the calculated vibrational spectra with experimental data revealed that adsorption at the bridge site is preferred at low coverage. At higher, catalytically more relevant coverages, the experimental spectra change dramatically and rather closely match the ab initio spectrum of benzene adsorbed at the hollow site. This change in site preference might be due to repulsive interactions between adsorbed species. Benzene adsorbed at the hollow sites can adsorb in a much more compact way without

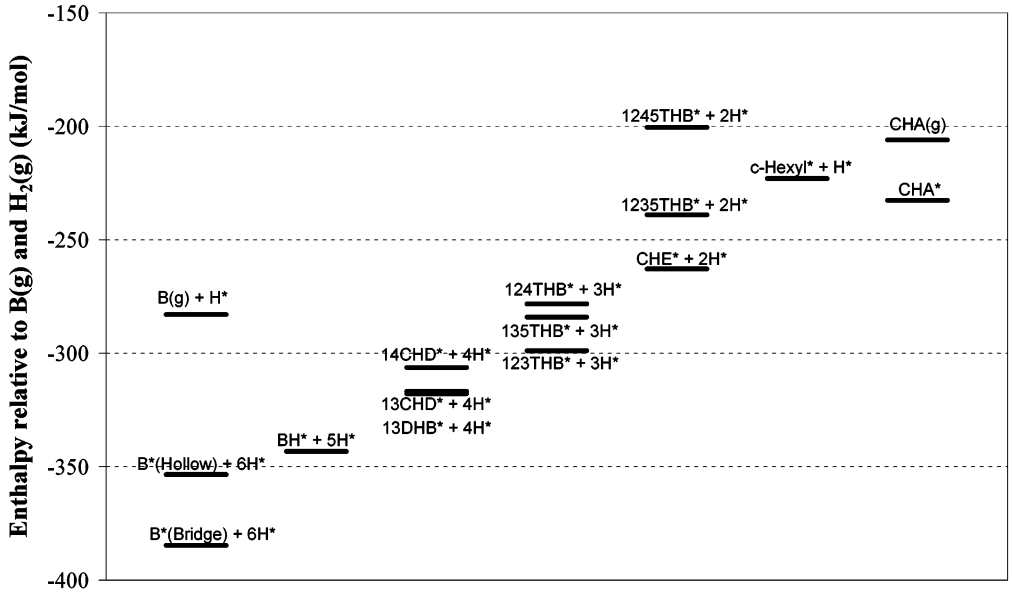

Figure 2. Enthalpy diagram for possible reactive intermediates during the hydrogenation of benzene. For species with different adsorption modes, only the catalytically significant mode was included.

overlap of the van der Waals spheres, which would lead to large repulsive interactions, as compared to benzene adsorbed at the bridge sites.[17] Moreover, the DFT calculations also revealed that hollow-site benzene has a low energy barrier for diffusion (∼5 kJ/mol) and is therefore very mobile, whereas benzene adsorbed at the bridge site has a much higher energy barrier for diffusion (∼50 kJ/mol).[10] The corresponding entropy difference between the two adsorption modes might also favor the hollow-site species at higher temperatures.

Hydrogen adsorption on Pt(111) is one of the most studied systems, both experimentally and theoretically (e.g., ref 12). Hydrogen dissociatively adsorbs, forming two coadsorbed hydrogen atoms. At low coverages, dissociative adsorption enthalpies between −60 and −90 kJ/mol have been reported. Surface science and most theoretical studies indicate that the resulting hydrogen atoms sit at fcc hollow sites. However, both experiment and theory find that atomically adsorbed hydrogen is highly mobile. Indeed, DFT studies report a very small difference between the adsorption energies for the hollow and for the top site (∼5 kJ/mol).[51] Our calculations yield a low coverage dissociative adsorption energy of −85 kJ/mol for the hollow site and of −94 kJ/mol for the top site, in agreement with the lower range of the experimental adsorption energies, and confirm the high mobility of the adsorbed hydrogen atom, with a diffusion barrier of only 5 kJ/mol.

14CHD adsorption was discussed in detail in ref 11. Three possible adsorption modes were identified: quadra-σ adsorption at the bridge site with an adsorption energy of −146 kJ/mol, π-di-σ bonding at the hollow site with a slightly lower adsorption energy of −142 kJ/mol, and a di-π mode at the bridge site with an adsorption energy of only −88 kJ/mol. On the basis of semiempirical valence bond theory, Koel et al.[18] have proposed a value of −144 kJ/mol for the adsorption energy. No experimental values are available because CHD readily dehydrogenates during temperature-programmed reaction (TPR).

Also three adsorption modes were identified for 13CHD:[13] 1,2-π-3,4-di-σ adsorption at the bridge site is the preferred mode with an adsorption energy of −155 kJ/mol; 1,4-di-σ-2,3-π adsorption at the hollow site has an adsorption energy of −147 kJ/mol. Ring strain makes 1,4-di-σ-2,3-π adsorption at the bridge site unfavorable ($E_{ads} = -75$ kJ/mol).[13]

Five different adsorption modes have been found for CHE.[13] The favored geometry, boat-di-σ, has a calculated adsorption energy of −81 kJ/mol, in fairly good agreement with a reported experimental value of −72 kJ/mol.[19]

The *CHA adsorption* energy of −27 kJ/mol is low as compared to experimental values (around −58 kJ/mol).[20−22] CHA interacts with the catalyst via 3 C−H···Pt bonds. This type of weak interaction has been shown to be at least in part due to dispersive forces,[52] which are not treated accurately by DFT.[44] Though similar interactions are also found for other molecules discussed here, it is far more important for closed shell alkanes such as CHA.

The radical *π-allylic cyclohexenyl (123THB)* has been found to be rather stable during the dehydrogenation of CHE[19,23,25−28] and CHA[20,25,29] and has been characterized by HREEL,[20,23] SFG,[28] and RAIR[25] spectroscopy. The calculated geometry of the adsorbed cyclohexenyl species (Figure 3) can be compared qualitatively with the spectroscopic data. Two distinct bands are found in the C−H stretching region of the RAIRS and SFG spectra of 123THB. Manner et al.[25] assigned the lower peak (at 2846 cm^{-1}) to a symmetric CH_2 stretch of the two symmetric methylene groups. This frequency is slightly lower than the symmetric CH_2 stretching frequency in cyclohexene (2846 vs 2864 cm^{-1}), consistent with the slightly longer (weaker) C−H bond length (111.3 pm) found in the calculation. A correlation between calculated C−H bond length and the frequency shift has also been observed for adsorbed 14CHD.[11] More importantly, Manner et al. assigned the sharp high-frequency peak (at 2930 cm^{-1}) as indirect evidence for an agostic, i.e., hydrogen-bond like, C−H···Pt interaction. Such an interaction is clearly found in the calculated structure (Figure 3). Unfortunately, no softened mode vibrations were observed in the experimental spectrum, probably because the band is too broad.[25] Such modes would provide more direct evidence for a H···Pt interaction.

In general it can be concluded that DFT provides a reasonably accurate description of the adsorption of unsaturated hydrocarbons on Pt(111), with adsorption energies typically within 10−20 kJ/mol of experimental data.

The data in Table 1 allow the construction of an enthalpy diagram for the possible surface intermediates (Figure 2). To simplify the diagram, only the enthalpy levels for the preferred

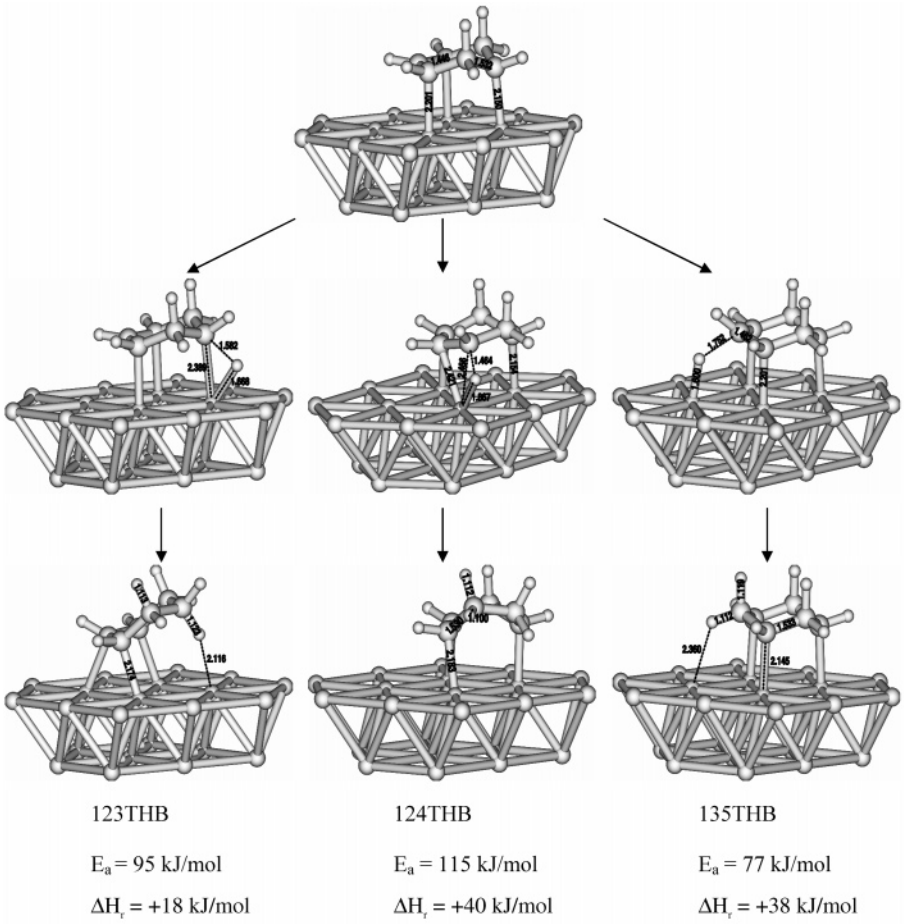

Figure 3. Three reaction paths for the third hydrogenation step starting from 13DHB. The acronyms of the intermediates, the hydrogenation activation energies, and reaction enthalpies (kJ/mol) are listed. Bond distances are reported in Å.

adsorption modes are shown in Figure 2. For benzene, however, both hollow- and bridge-site adsorption are included. Figure 2 qualitatively agrees with the semiempirical energy diagram for cyclohexane dehydrogenation proposed by Koel et al.,[18] though important differences are observed. In particular for the radical species, Koel et al. propose higher adsorption energies. This is related to their value of the C−Pt bond strength of 220 kJ/mol. This value is significantly higher than the calculated adsorption energy of *c*-hexyl, 167 kJ/mol. Also the strength of the di-σ bond in 123THB might be lower than in CHE. In particular, for BH* their adsorption energy of −365 kJ/mol is much higher than the ab initio value, −229 kJ/mol. Analogous differences are found for 123THB (−294 vs −203 kJ/mol) and *c*-hexyl (−220 vs −167 kJ/mol).

Adsorbed benzene and six adsorbed hydrogen atoms form the thermodynamic sink in the reaction system. Thermodynamically, B* and H* can be expected to be the dominant species on the catalyst surface and may likely be the most-abundant reaction intermediate (MARI). This assumes, however, that the governing surface intermediate concentrations are controlled by thermodynamics rather than by kinetics.

Contrary to gas-phase hydrogenation, the catalytic hydrogenation over Pt(111) is an endothermic process. In particular, the strong H−Pt bond seems to cause the endothermicity. Each of the subsequent hydrogen addition steps requires breaking a strong H−Pt bond (265 kJ/mol, Table 1) and a strong C−Pt bond (about 165 kJ/mol, e.g., *c*-hexyl in Table 1) in order to form a C−H bond (∼400 kJ/mol). As a result, all of the hydrogenation steps from B*(bridge) + 6H* to *c*-hexyl* + H* are comparable with reaction enthalpies that are ∼30 kJ/mol endothermic. Contrary to the first five hydrogenation steps, the sixth hydrogenation step is found to be exothermic. Though CHA is completely saturated, it still binds to Pt with a calculated adsorption energy of −27 kJ/mol. Such bonding is typical for CHA, thus leading to the last hydrogenation step being exothermic. Without this interaction, the *c*-hexyl hydrogenation would be endothermic (+16 kJ/mol).

The enthalpy diagram can also provide preliminary ideas on the presence and potential identity of a rate-determining step. This is speculative though, since identifying the true rate-determining steps would require a full analysis of the reaction rate coefficients as well as the surface coverages. Previously,[6] we used a limited enthalpy diagram (considering only adsorbed hollow-site benzene, CHD, CHE, and CHA) to speculate that the third or fourth hydrogen addition may be rate-limiting. Indeed, the hydrogenation from cyclohexadiene to cyclohexene is more endothermic (+55 kJ/mol) than the hydrogenation from hollow-site benzene to cyclohexadiene (+36 kJ/mol) or from cyclohexene to cyclohexane (+30 kJ/mol). Hence, if the activation energies are assumed to follow an Evans-Polanyi relation and thus scale with the enthalpy of reaction, it can be expected that the third or fourth hydrogenation step has the highest barrier.

These arguments can now be further extended to the more detailed enthalpy diagram derived in this section (Figure 2). Since the first five steps have very similar endothermic heats of reaction, it might be speculated that they have very similar activation barriers. Similarly, the activation energy for the last hydrogenation step can then be assumed to be significantly lower since this step is fairly exothermic.

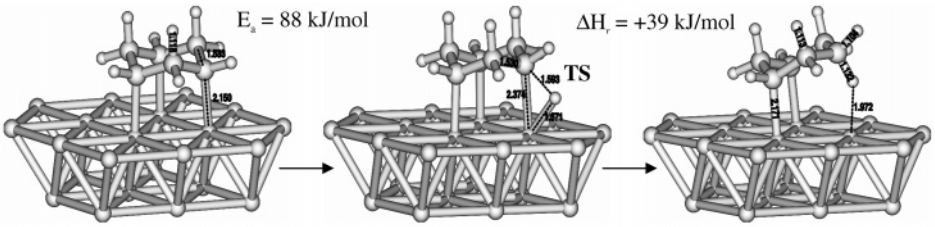

Figure 4. Reaction path for the fourth hydrogenation step starting from 135THB. Hydrogenation activation energies and reaction enthalpies are reported in kJ/mol, bond distances in Å.

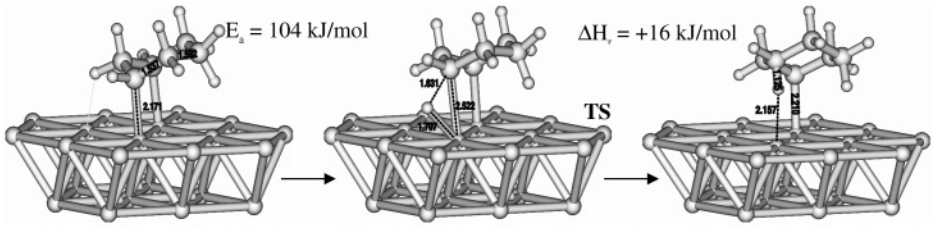

Figure 5. Reaction path for the fifth hydrogenation step starting from 1235THB. Hydrogenation activation energies and reaction enthalpies are reported in kJ/mol, bond distances in Å.

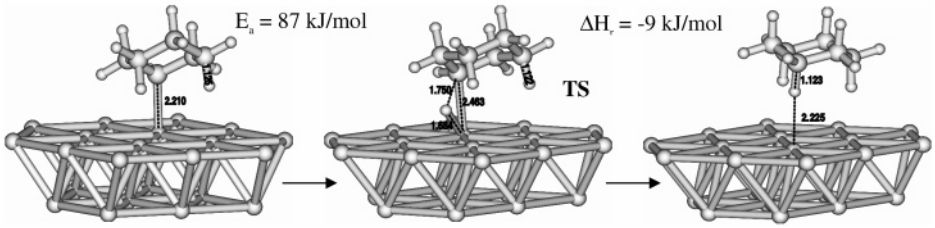

Figure 6. Reaction path for the final hydrogenation step starting from *c*-hexyl. Hydrogenation activation energies and reaction enthalpies are reported in kJ/mol, bond distances in Å.

As indicated, under catalytic conditions benzene adsorbed at the hollow site might be the dominant surface species. A more careful look at the reaction enthalpies starting from hollow-site benzene and considering the thermodynamically favored intermediates yields values of +10, +26, +18, +36, +40, and −10 kJ/mol, respectively. On the basis of the reaction enthalpies of the individual steps, the highest activation energy might be expected for the fourth or fifth step.

3.2. Activation Energies and Reaction Path Analysis. On the basis of the thermodynamic arguments of the previous section, it is difficult to establish the presence of a dominant reaction path. Though it is unlikely that, based on the enthalpy diagram in Figure 2, the dominant reaction path proceeds via the 1245THB* intermediate, the reaction enthalpy diagram does not allow one to select the most likely reaction path. Moreover, it was shown previously that the kinetics do not always follow thermodynamics for catalytic hydrogenation reactions, in that a less endothermic reaction does not always have a lower activation energy.[12] As a result, the Evans-Polanyi relationship does not always hold for catalytic hydrogenation reactions. To assess the presence of a dominant reaction path and of a possible rate-determining step, the activation energies were calculated for a number of carefully selected reaction steps. The location of a transition state is computationally rather demanding (see Computational Methods section). To reduce the number of transition state calculations, only the activation energies are calculated for the hydrogenation of a species that was formed via the dominant reaction path for the previous hydrogenation steps. For example, for the hydrogenation of BH*, three possible reactions paths were distinguished in Figure 1. Activation energies were calculated for all of these possible paths. If one of the activation energies is significantly lower than the other, this path may likely be considered the dominant reaction path for the hydrogenation of this species (e.g., hydrogenation to form 13DHB). The difference in activation energy should be at least 15 kJ/mol to correspond to a 50-fold difference in reaction rate at 450 K, assuming similar preexponential factors. The geometries of the transition states for the possible reaction paths are rather comparable (Figures 3−6) and similar preexponential factors can therefore be expected. If there is a dominant reaction path (e.g., forming 13DHB), only the hydrogenation reactions starting from the molecule formed via this dominant reaction path are considered in the next hydrogenation step.

Because the reaction enthalpies, ΔH_r(surface), were calculated by combining DFT adsorption energies with experimental or CBS-QB3* ab initio gas-phase reaction enthalpies, eq 1, the difference between the DFT activation energies for hydrogenation, E_a(hydro,DFT), and dehydrogenation is not equal to the reaction enthalpy of eq 1. Hence, if the hydrogenation activation energies are obtained from the DFT calculations, the dehydrogenation activation energies should be calculated using eq 2 to establish thermodynamic consistency.

$$E_a(\text{dehydro}) = E_a(\text{hydro,DFT}) - \Delta H_r(\text{surface}) \qquad (2)$$

The resulting dehydrogenation activation energies, E_a(dehydro), will differ from the DFT dehydrogenation activation energies. Alternatively, the DFT dehydrogenation activation energies can be applied. Then the hydrogenation activation energies have to be calculated using a relation similar to eq 2 to establish thermodynamic consistency. The latter procedure will, in general, yield higher activation energies by about 25 kJ/mol. Based on transition state theory it can be shown that the former procedure, i.e., using DFT hydrogenation activation

energies and calculating the dehydrogenation energies from eq 2, should be preferred.[12]

Next, the hydrogenation steps are discussed step by step. The results are summarized in Figure 1. The mechanism for the first two hydrogenation steps has been discussed in detail in our previous communication.[12] Benzene can adsorb at the hollow as well as the bridge sites. The hydrogenation from both of these adsorption modes was considered. For benzene adsorbed at the bridge site, two types of carbon−platinum bonds can be distinguished, leading to two distinct reaction paths.[12] The first reaction path is characterized by a two-step "three-centered mechanism" (H−Pt−C)[12] whereby the attacking H-atom moves over a Pt-atom while forming the C−H bond. The second reaction path resembles more a "slip mechanism" whereby a C═C bond slides upward to form a five-centered like (Pt−C−C−H−Pt) transition state. This is similar to what is seen for ethene hydrogenation.[40] Both mechanisms were observed for the other hydrogenation steps in this study as well. In general, for the reactions studied here the three-centered mechanism is found to have a lower activation energy than the slip mechanism. For the hydrogenation of bridge-site adsorbed benzene, activation barriers of 100 and 106 kJ/mol and reaction enthalpies of +51 and +42 kJ/mol were calculated, respectively. For benzene adsorbed at the hollow site, the six carbon−platinum bonds are symmetrically equivalent and there is only one reaction path. The hydrogenation of the less strongly bound hollow-site species has a lower activation energy at 74 kJ/mol and a reaction enthalpy of +10 kJ/mol. Because of the 26 kJ/mol lower activation energy, the weakly adsorbed hollow-site benzene is more likely to be the reactive species, whereas the bridge-site species may be too strongly adsorbed and can thus be considered as a spectator species. For ethene hydrogenation, similar behavior has been found experimentally on ideal (111) surfaces[37] and on model catalysts,[38] as well as theoretically from DFT calculations.[2,39] Ethene adsorption in the di-σ mode is much stronger than in the π-mode. Based on sum frequency generation (SFG) studies, Somorjai and co-workers proposed that the weakly π-bound ethene is the reactive species, whereas the strongly adsorbed di-σ species is mostly converted to a site-blocking ethylidyne species.[37] Though the π-bound ethene was stated to have a surface concentration of only 4%, it was found to be the reactive species. At low coverages, hollow-site benzene is also a minority species, but the relative surface concentrations of the hollow- and the bridge-site benzene were found to vary strongly with coverage, probably due to the lower repulsive interactions for the hollow-site species.[10,15,17] At temperatures, pressures, and coverages that are consistent with industrial hydrogenation conditions, the more reactive hollow-site species may become the more important surface species.

The difference in activation energy between hollow- and bridge-site hydrogenation, 26 kJ/mol, is sufficient to consider hydrogenation of the hollow-site species as the dominant reaction path. Therefore, only the cyclohexadienyl species (BH*) formed from hollow-site benzene hydrogenation was considered in the second hydrogenation step. Because of the low symmetry of adsorbed BH, five possible hydrogenation paths can be distinguished: two leading to 13CHD, two leading to 13DHB, and one leading to 14CHD.[12] The preferred mechanism for hydrogenation of BH to 13CHD has a barrier of 91 kJ/mol; hydrogenation to 14CHD has an activation energy of 115 kJ/mol. The dominant reaction path leads to 13DHB with a barrier of 72 kJ/mol and follows a three-centered mechanism. On the basis of the enthalpy diagram of Figure 2, one would expect much smaller differences in activation energy between the reaction paths. Clearly, the activation energies are not uniquely determined by the reaction enthalpy, but also depend on the specific details of the reaction mechanism.

A reaction path analysis of the first two steps can be compared to experimental surface science data for the adsorption and dehydrogenation of cyclohexadienes on Pt(111). Because surface science studies are primarily carried out in UHV, dehydrogenation studies are most convenient. In refs 11 and 12, it was found that our ab initio results can be used to begin to explain the surface science results. The calculated barrier for 13CHD dehydrogenation, 52 kJ/mol (Figure 1), is within the experimental range, 50−69 kJ/mol.[25,40−42] Surface science studies indicate that 14CHD dehydrogenates more slowly than 13CHD, with a barrier between 65 and 74 kJ/mol,[25,40,42] again in reasonable agreement with the ab initio barrier of 78 kJ/mol.

The next step along the dominant reaction path is the hydrogenation of 13DHB. Three possible reaction paths were found. The reactants, transition states, and products for the three reaction paths are shown in Figure 3. Activation energies of 77 kJ/mol (135THB), 95 kJ/mol (cyclohexenyl, 123THB), and 115 kJ/mol (124THB) were calculated. Note that the preferred reaction path is rather endothermic, by +38 kJ/mol. 135THB and 123THB are formed via a three-centered mechanism, whereas the mechanism leading to 124THB resembles more the slip mechanism. This mechanistic difference can in part explain the higher barrier for the latter reaction. The kinetics do not follow thermodynamics for the third hydrogenation step, since adsorbed 123THB is 20 kJ/mol more stable than 135THB, but the corresponding hydrogenation barrier is 18 kJ/mol higher. As a consequence, the dehydrogenation barrier of 123THB is rather high at 77 kJ/mol (Figures 1 and 3) and 123THB is rather stable during the dehydrogenation of CHA, in agreement with the surface science results discussed above. The difference in activation energies between the preferred and the alternative paths is again substantial (18 kJ/mol), and the dominant reaction path goes via 135THB. As a consequence, the formation of cyclohexene during benzene hydrogenation is expected to be at best a side reaction, since 135THB hydrogenation does not lead to CHE (Figure 1). This observation is consistent with early observations by Tetenyi and Paal.[3] On the basis of extensive radiotracer studies of benzene hydrogenation, these authors found that "the reaction path which cannot lead to cyclohexene" should be "regarded as more or less favored".

Along the preferred reaction path, the hydrogen atom adds in the meta position of the methylene groups, as was also observed for the addition of the second hydrogen atom. The barrier for the third addition, 77 kJ/mol, is similar to the barriers for the first and the second hydrogenation of 74 and 72 kJ/mol, respectively. The higher barrier for hydrogenation in the ortho or para position of a methylene group might be due to the strength of the σ_{C-Pt} bond at these positions. Indeed, in the corresponding gas-phase structures, carbon atoms in the ortho and para position of the methylene group have more pronounced radical character. The C−Pt bond at these positions will therefore be stronger. It seems that the strength, or rather the weakness, of the breaking C−Pt bond determines the dominant reaction path.

The rather high dehydrogenation barrier of the adsorbed π-allylic cyclohexenyl (123THB) is consistent with the observed stability during TPR studies. Using TPR, Pettiette-Hall et al.[24] determined a barrier of 74 kJ/mol for the dehydrogenation of 123THB. A slightly higher value of 87 kJ/mol was put forward

by Henn et al.[23] The calculated dehydrogenation barrier of 77 kJ/mol again shows good agreement with the experimental values.

Only one reaction path appears to be available for the hydrogenation of 135THB (Figure 4). A three-centered mechanism is found and the barrier, 88 kJ/mol, is significantly higher than for the first three steps. The hydrogen addition can only occur in the ortho position of the methylene groups. The barrier is comparable to the barriers leading to 123THB (95 kJ/mol) and 13CHD (91 kJ/mol) and seems characteristic for hydrogen addition in the meta position of a methylene group. The length of the C−Pt bond which needs to be broken and the geometry of the transition state are also very similar to the latter reactions. The reaction is +39 kJ/mol endothermic and an important agostic H···Pt interaction with the surface is observed in the product 1235THB. The H···Pt distance is rather short at 197 nm. As a result, the C−H bond length increases from ∼110 to 113.2 pm in the product. Similar but less strong interactions are responsible for the CHA adsorption enthalpy of −27 kJ/mol. In CHA, the H···Pt distance is 223 nm and the axial C−H bond length increases to 112.3 nm.

The fifth hydrogenation barrier is even higher at 104 kJ/mol. This value seems slightly high, as compared to the barrier of the fourth step. Here too, hydrogenation occurs in the ortho position of two methylene groups. This high barrier is quite interesting since the reaction is only +16 kJ/mol endothermic. The high barrier might be related to the breaking of the important H···Pt agostic interaction in 1235THB during the hydrogenation step. In the transition state, this interaction has to be overcome, thereby increasing the barrier. The strength of this interaction can be estimated from the difference in adsorption energy between the chair- and the boatlike conformation of 1235THB, i.e., 26 kJ/mol. Indeed, this agostic interaction is absent in the boatlike conformation.

Figure 6 shows the reaction mechanism for the addition of the sixth hydrogen atom, yielding adsorbed CHA. Again a three-centered mechanism is found. The transition state geometry is similar to the fourth hydrogenation step. Also the barrier is similar, at 87 kJ/mol. No evidence of a H···Pt interaction can be found in the reactant, *c*-hexyl. As discussed in the previous section, the last hydrogenation step is exothermic by 9 kJ/mol and it is the only exothermic step along the catalytic hydrogenation path. The corresponding dehydrogenation barrier of CHA is 96 kJ/mol, or 69 kJ/mol if gas-phase CHA is taken as a reference. These values are consistent with results from other theoretical studies of alkane dehydrogenation/alkyl hydrogenation over Pt(111). For methyl hydrogenation, a barrier of 71 kJ/mol was calculated on Pt(111).[52] For the reverse dehydrogenation reaction, a barrier of 64 kJ/mol was reported. For ethyl hydrogenation on Pd(111) a barrier of 71 kJ/mol has been calculated.[54] For the corresponding ethane dehydrogenation, a barrier of 76 kJ/mol was found.

There is ample experimental evidence that alkane activation is a difficult step. Because saturated alkanes are quite stable, the scission of one of the C−H bonds is often the rate-limiting step for alkane dehydrogenation.[55] Experimental studies of CHA dehydrogenation on a Pt(111) surface on the other hand, report lower values for the activation barrier of CHA dehydrogenation. Various authors[20−22,30−32] report values in the range 40-60 kJ/mol. The low value might be related to defects which can speed up the dehydrogenation reaction considerably. This is consistent with the structure sensitivity reported for CHA dehydrogenation reactions by some authors.[27,34] This structure sensitivity might seem odd at first sight, since dehydrogenation is the reverse elementary reaction of hydrogenation, which is found not to be structure-sensitive. However, if one considers the very high mobility of CHA, it can be envisioned that CHA may rapidly diffuse to a defect site. However, some researchers have also reported that CHA dehydrogenation is a structure-insensitive reaction.[56] The dehydrogenation of CHA might also be assisted by coadsorbed hydrogen. Perry and Hemminger[33] reported that coadsorbed hydrogen can lower the activation energy for CHA dehydrogenation by approximately 20%.

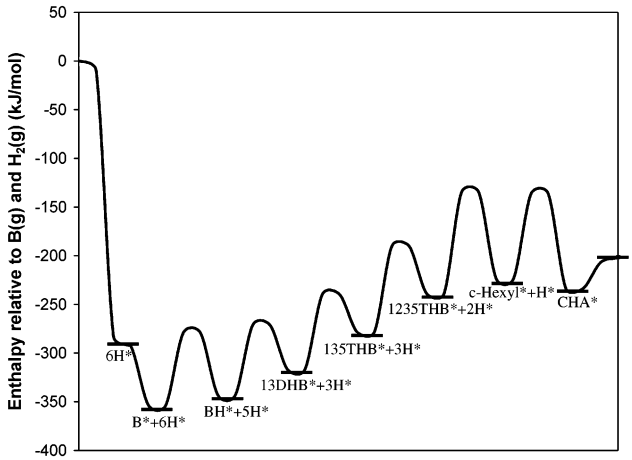

Figure 7. Energy profile along the dominant reaction path.

The reaction path analysis presented here unravels details of the reaction mechanism (Figure 1) and can provide some answers to the questions raised in the Introduction. In Figure 7, the calculated energy diagram for the dominant reaction path is shown. The activation energies along this path are significantly lower than along any other path. This dominant reaction path does not pass via cyclohexadiene nor cyclohexene; instead, hydrogen prefers to add in the meta position of a methylene group. Note that the second and third hydrogenation steps determine the dominant reaction path (Figure 1). Indeed, only one possible reaction path is available for the hydrogenation of 135THB. The only product that can desorb is cyclohexane, since neither CHE nor CHD is formed along the predominant path.

Two categories of activation energies are found: low barriers at ∼75 kJ/mol for the first three hydrogenation steps, and higher barriers of ∼88 kJ/mol for steps four and six. The highest barrier at 104 kJ/mol is calculated for the fifth hydrogenation step. The higher value for this barrier is likely the result of a H···Pt interaction in the reactant for this step, which increases its barrier by ∼15 kJ/mol. Because of their lower barriers, steps 1, 2, 3, and 4 may be assumed quasi-equilibrated. Step 5 has a considerably higher barrier and may be the rate-limiting step. This of course will depend on the values of the preexponential factors also, as well as of the relative surface coverages. However, from the similarity in the reaction mechanisms and transition state structures for the different hydrogenation steps along the dominant reaction path, rather similar values might be expected for the former. Hence, the reaction rate coefficients are expected to be governed by the activation energies. The reverse reaction of the sixth step has a fairly high activation barrier and may not be quasi-equilibrated. However, the relatively facile and irreversible CHA desorption may make the reverse dehydrogenation reaction kinetically unimportant.

From the energy profile in Figure 7 it can be seen that the highest point along the dominant reaction path is the transition state of the fifth hydrogenation step, but the transition state of the sixth hydrogenation step is only 2 kJ/mol lower. These steps may be the rate-determining steps for benzene hydrogenation.

The thermodynamic sink of the energy profile is clearly the adsorbed benzene and hydrogen (Figure 7). They are likely to be the most-abundant reaction intermediates (MARI).

The analysis in the previous paragraphs has been based on the energy profile. Clearly, a more definite assessment of the presence of a rate-determining step and a most-abundant reaction intermediate requires the calculation of reaction entropies and preexponential factors, next to the enthalpies and activation energies presented here. Moreover, to take into account the effect of surface concentrations, a full microkinetic analysis should also be performed. However, the analysis presented in this paper does give very strong indications of the presence of a dominant reaction path, a rate-determining step, and a most-abundant reaction intermediate for the catalytic hydrogenation of aromatic molecules. These powerful concepts can be used as a guideline to the kineticist for the construction of a kinetic model for the catalytic hydrogenation of aromatics.

4. Conclusions

Ab initio DFT calculations were performed to analyze the reaction path for benzene hydrogenation to cyclohexane. The results can be articulated into three main conclusions.

(i) A dominant reaction path was found, along which activation energies for every step are lower than for alternative reaction paths. Along the dominant reaction path, hydrogen atoms add in the meta position of each other. Hence, this dominant reaction path does not pass via cyclohexadiene nor cyclohexene. The only product along the dominant reaction path that can desorb is cyclohexane.

(ii) The calculated activation energies for the first three steps are ~75 kJ/mol, while those for the fourth and sixth hydrogen additions have barriers of ~88 kJ/mol. The highest barrier, 104 kJ/mol, was found for the fifth hydrogenation step. This is at least 16 kJ/mol higher than for the other steps. At 400 K, a typical temperature for aromatic hydrogenation, such a difference in activation energies corresponds to a 100-fold difference in reaction rate coefficient and the fifth hydrogen addition may be *rate-determining*. Benzene and hydrogen adsorption and first four hydrogen additions are likely quasi-equilibrated, while cyclohexane desorption and, consequently, the sixth hydrogenation step can be considered irreversible.

(iii) Adsorbed benzene and hydrogen are found to be significantly more stable than the other reaction intermediates. They are likely to be the *most-abundant reaction intermediates*.

The results from the ab initio reaction path analysis refine our knowledge on the hydrogenation mechanism on a molecular level and provide valuable information for the construction of a kinetic model for the catalytic hydrogenation of aromatic molecules.

Acknowledgment. M.S. is grateful to the Fund for Scientific Research-Flanders, Belgium (F.W.O.-Vlaanderen) for a Research Assistantship.

References and Notes

(1) Cooper, B. H.; Donnis, B. B. L. *Appl. Catal. A: Gen.* **1996**, *137*, 203.
(2) Neurock, M. *J. Catal.* **2003**, *216*, 73.
(3) Tétényi, P.; Paal, Z. *Z. Phys. Chem. N. F.* **1972**, *80*, 63.
(4) Tétényi, P. *J. Catal.* **1994**, *147*, 601.
(5) Lin, S. D.; Vannice, M. A. *J. Catal.* **1993**, *143*, 563.
(6) Thybaut, J. W.; Saeys, M.; Marin, G. B. *Chem. Eng. J.* **2002**, *90*, 117.
(7) Van Meerten, R. Z. C.; Coenen, J. W. E. *J. Catal.* **1977**, *46*, 13.
(8) Lindfors, L. P.; Salmi, T. *Ind. Eng. Chem. Res.* **1993**, *32*, 34.
(9) Chou, P.; Vannice, M. A. *J. Catal.* **1997**, *107*, 140.
(10) Saeys, M.; Reyniers, M.-F.; Neurock, M.; Marin, G. B. *J. Phys. Chem. B* **2002**, *106*, 7489.
(11) Saeys, M.; Reyniers, M.-F.; Neurock, M.; Marin, G. B. *Surf. Sci.* **2002**, *513*, 315.
(12) Saeys, M.; Reyniers, M.-F.; Neurock, M.; Marin, G. B. *J. Phys. Chem. B* **2003**, *107*, 3844.
(13) Saeys, M. Ph.D. Thesis, Ghent University, 2002.
(14) Campbell, J. M.; Seimanides, S. G.; Campbell, C. T. *J. Phys. Chem.* **1989**, *93*, 815; Xu, C.; Tsai, Y.-L.; Koel, B. E. *J. Phys. Chem.* **1994**, *98*, 585.
(15) Haq, S.; King, D. A. *J. Phys. Chem.* **1996**, *100*, 16957.
(16) Morin, C.; Simon, D.; Sautet, P. *J. Phys. Chem. B* **2003**, *107*, 2995.
(17) Held, G. *J. Phys.: Condens. Mater.* **2003**, *15*, R1501.
(18) Koel, B. E.; Blank, D. A.; Carter, E. A. *J. Mol. Catal. A: Chem.* **1998**, *131*, 39.
(19) Xu, C.; Koel, B. E. *Surf. Sci.* **1994**, *304*, 249.
(20) Bussell, M. E.; Henn, F. C.; Campbell, C. T. *J. Phys. Chem.* **1992**, *96*, 5978.
(21) Rodriguez, J. A.; Campbell, C. T. *J. Phys. Chem.* **1989**, *93*, 826.
(22) Pansoy-Hjelvik, M. E.; Schnabel, P.; Hemminger, J. C. *J. Phys. Chem. B* **2000**, *104*, 6554.
(23) Henn, F. C.; Diaz, A. L.; Bussell, M. E.; Hugenschmidt, M. B.; Domagala, M. E.; Campbell, C. T. *J. Phys. Chem.* **1992**, *96*, 5965.
(24) Pettiette-Hall, C. L.; Land, D. P.; McIver, R. T.; Hemminger, J. C. *J. Am. Chem. Soc.* **1991**, *113*, 2755.
(25) Manner, W. L.; Girolami, G. S.; Nuzzo, R. G. Sequential Dehydrogenation of Unsaturated Cyclic C5 and C6 Hydrocarbons on Pt(111). *J. Phys. Chem. B* **1998**, *102*, 10295.
(26) Henn, F. C.; Diaz, A. L.; Bussell, M. E.; Hugenschmidt, M. B.; Domagala, M. E.; Campbell, C. T. *J. Phys. Chem.* **1992**, *96*, 5965.
(27) McCrea, K. R.; Somorjai, G. A. *J. Mol. Catal. A: Chem.* **2000**, *163*, 43.
(28) Su, X.; Kung, K.; Lahtinen, J.; Shen, R. Y.; Somorjai, G. A. *Catal. Lett.* **1998**, *54*, 9.
(29) Demuth, J. E.; Ibach, H.; Lehwald, S. *Phys. Rev. Lett.* **1978**, *40*, 1044.
(30) Holmes-Parker, D.; Pettiette-Hall, C. L.; Li, Y. Z.; McIver, R. T.; Hemminger, J. C. *J. Phys. Chem.* **1992**, *96*, 1888.
(31) Land, D. P.; Erley, W.; Ibach, H. *Surf. Sci.* **1993**, *289*, 237.
(32) Pettiette-Hall, C. L.; Land, D. P.; McIver, R. T.; Hemminger, J. C. *J. Am. Chem. Soc.* **1991**, *113*, 2755.
(33) Perry, D. A.; Hemminger, J. C. *J. Am. Chem. Soc.* **2000**, *112*, 8079.
(34) Herz, R. K.; Gillespie, W. D.; Petersen, E. E.; Somorjai, G. A. *J. Catal.* **1981**, *67*, 371.
(35) Horiuti, J.; Polanyi, M. *Trans. Faraday Soc.* **1934**, *30*, 1164.
(36) Dobert, F.; Gaube, J. *Chem. Eng. Sci.* **1996**, *51*, 2873; Struijk, J.; Moene, R.; Vanderkamp, T.; Scholten, J. J. F. *Appl. Catal. A.: Gen.* **1995**, *89*, 77; Struijk, J.; Dangremond, M.; Lucasderegt, W. J. M.; Scholten, J. J. F. *Appl. Catal. A.: Gen.* **1992**, *83*, 263.
(37) Somorjai, G. A.; Rupprechter, G. *J. Phys. Chem. B* **1999**, *103*, 1623.
(38) Freund, H.-J.; Bäumer, M.; Libuda, J.; Risse, T.; Rupprechter, G.; Shaikhutdinov, S. *J. Catal.* **2003**, *216*, 223.
(39) Neurock, M.; Pallassana, V.; van Santen, R. A. *J. Am. Chem. Soc.* **2000**, *122*, 1150.
(40) Hugenschmidt, M. B.; Diaz, A. L.; Campbell, C. T. *J. Phys. Chem.* **1992**, *96*, 5974.
(41) Peck, J. W.; Koel, B. E. *J. Am. Chem. Soc.* **1996**, *118*, 2708.
(42) Su, X.; Shen, Y. R.; Somorjai, G. A. *Chem. Phys. Lett.* **1997**, *280*, 302.
(43) Boudart, M. *AIChE J.* **1972**, *18*, 465; Boudart, M.; Djéga-Mariadassou, G. *Kinetics of Heterogeneous Catalytic Reactions*; Princeton University Press: Princeton 1984; Djéga-Mariadassou, G.; Boudart, M. *J. Catal.* **2003**, *216*, 89.
(44) Koch, W.; Holthausen, M. C. *A Chemist's Guide to Density Functional Theory*, 2nd Ed.: Wiley-VCH: Weinheim, 2001.
(45) te Velde, G.; Bickelhaupt, F. M.; Baerends, E. J.; Fonseca Guerra, C.; Van Gisbergen, S. J. A.; Snijders, J. G.; Ziegler, T. *J. Comput. Chem.* **2001**, *22*, 931.
(46) Somorjai, G. A. *Introduction to Surface Chemistry and Catalysis*; Wiley: New York, 1994.
(47) Saeys, M.; Reyniers, M.-F.; Van Speybroeck, V.; Waroquier, M.; Marin, G. B. *J. Phys. Chem. A* **2003**, *107*, 9147.
(48) Montgomery, J. A., Jr.; Frisch, M. J.; Ochterski, J. W.; Petersson, G. A. *J. Chem. Phys.* **2000**, *112*, 6532.
(49) Frisch, M. J.; Trucks, G. W.; Schlegel, H. B.; Scuseria, G. E.; Robb, M. A.; Cheeseman, J. R.; Zakrzewski, V. G.; Montgomery, J. A., Jr.; Stratmann, R. E.; Burant, J. C.; Dapprich, S.; Millam, J. M.; Daniels, A. D.; Kudin, K. N.; Strain, M. C.; Farkas, O.; Tomasi, J.; Barone, V.; Cossi, M.; Cammi, R.; Mennucci, B.; Pomelli, C.; Adamo, C.; Clifford, S.; Ochterski, J.; Petersson, G. A.; Ayala, P. Y.; Cui, Q.; Morokuma, K.; Malick, D. K.; Rabuck, A. D.; Raghavachari, K.; Foresman, J. B.; Cioslowski, J.; Ortiz, J. V.; Baboul, A. G.; Stefanov, B. B.; Liu, G.; Liashenko, A.; Piskorz, P.; Komaromi, I.; Gomperts, R.; Martin, R. L.; Fox, D. J.; Keith, T.; Al-

Laham, M. A.; Peng, C. Y.; Nanayakkara, A.; Gonzalez, C.; Challacombe, M.; Gill, P. M. W.; Johnson, B.; Chen, W.; Wong, M. W.; Andres, J. L.; Head-Gordon, M.; Replogle, E. S.; Pople, J. A. *Gaussian 98*, rev. A.7; Gaussian, Inc.: Pittsburgh, PA, 1998.

(50) Afeefy, H. Y.; Liebman, J. F.; Stein, S. E. "Neutral Thermochemical Data" in NIST Chemistry WebBook, NIST Standard Reference Database Number 69, Linstrom, P. J., Mallard, W. G., Eds.; July 2001, National Institute of Standards and Technology, Gaithersburg MD, 20899 (http://webbook.nist.gov).

(51) Nobuhara, K.; Nakanishi, H.; Kasai, H.; Okiji *Surf. Sci.* **2001**, *493*, 271.

(52) Fosser, K. A.; Nuzzo, R. G.; Bagus, P. S.; Woll, C. *J. Chem. Phys.* **2003**, *118*, 5115.

(53) Michaelides, A.; Hu, P. *J. Am. Chem. Soc.* **2000**, *122*, 9866.

(54) Neurock, M.; van Santen, R. A. *J. Phys. Chem. B* **2000**, *104*, 11127.

(55) Zaera, F. *Appl. Catal. A* **2002**, *229*, 75.

(56) Sinfelt, J. H.; Carter, J. L.; Yates, D. J. C. *J. Catal.* **1972**, *24*, 283TS.